N-Substituted Poly(3,4-propylenedioxypyrrole)s: High Gap and Low Redox Potential Switching Electroactive and Electrochromic Polymers

Gürsel Sönmez,[†,‡] Irina Schwendeman,[†] Philippe Schottland,[†] Kyukwan Zong,[†] and John R. Reynolds*[,†]

Department of Chemistry, Center for Macromolecular Science and Engineering, University of Florida, Gainesville, Florida 32611-7200, and Faculty of Science and Letters, Department of Chemistry, Istanbul Technical University, 80626 Maslak, Istanbul, Turkey

Received July 15, 2002; Revised Manuscript Received November 18, 2002

ABSTRACT: A series of electrochromic N-substituted poly(3,4-propylenedioxypyrrole)s (PProDOPs) are reported, which exhibit the combined properties of a high (>3 eV) electronic band gap, colored oxidatively doped forms, and easily accessible, low redox potentials. Utilizing methyl (Me), propyl (Pr), octyl (Oct), propanesulfonated (PrS), and ethoxyethoxyethanol (Gly) pendants, the absorbance of the $\pi-\pi^*$ transition of the resulting polymers is blue-shifted when compared to the nonderivatized parent. For example, in the case of poly(*N*-ethoxyethoxyethanol ProDOP) (*N*-Gly PProDOP), this transition displays a maximum at 306 nm (onset at 365 nm), providing a colorless and highly transparent neutral polymer with a luminous transmittance greater than 99% for a film thickness of about 200 nm. N-Substituted PProDOPs display very well-defined cyclic voltammograms, with $E_{1/2} < -0.1$ V vs Fc/Fc^+ (+0.2 V vs SCE), negative of the oxidation of water, as desired for materials having stable doped forms and long-lived redox switching properties. In addition, the presence of a sulfonate group at the end of the propyl chain in *N*-PrS PProDOP offers the possibility of self-doping along with water solubility of the polymer. As a result, *N*-PrS PProDOP exhibits a fast and regular growth even in the absence of supporting electrolyte. This new family of polymers has not only shown interesting electrochromic properties in the visible. Upon doping, a very strong absorption is observed in the near-infrared (NIR) with changes in transmittance up to 97%, extending the use of these polymers as the active layer in vis−NIR switchable devices.

Introduction

Electrochromism provides reversible changes in a material's response to reflected or transmitted light via changes in redox states. Since its initial development in inorganic materials,[1] numerous organic and hybrid systems have been developed, exhibiting a broad array of colorimetric and electrochemical switching properties.[2] Electrochromic materials are presently useful for the construction of mirrors,[3] displays,[4,5] windows,[6−10] and earth-tone chameleon materials.[11−13] On the basis of this concept, electrochromic rearview[14,15] and exterior wing mirrors have been recently commercialized in the automotive industry utilizing molecular organic eletrochromes dissolved in an ionic gel.

Conducting electroactive polymer (CEP)-based electrochromics have received increasing attention due to their potential for facile processing, structurally controllable states, high contrasts, fast switching speeds, and ability to be applied to flexible eletrochromic devices.[16−18] By controlling the electronic character of the extended π system along the neutral polymer backbone, the $\pi-\pi^*$ transition can be adjusted across the electromagnetic spectrum from the UV, through the visible and into the near-infrared. Oxidative or reductive doping is used to generate charge carriers with optical transitions at lower energies; thus, significant color changes are observed. In addition, conjugated electrochromic polymers can offer outstanding coloration efficiencies and fast switching times, as exhibited by poly(3,4-alkylenedioxythiophene) (PXDOTs) derivatives.[19,20] An important aspect of the PXDOTs, along with the structurally similar poly(3,4-alkylenedioxypyrrole)s (PXDOPs), is their ability to switch from deeply colored neutral states to highly transmissive (essentially transparent as thin films) doped states. Other benefits are their ability to produce multiple colors within the same material,[13] and the colors attained can be tuned through modification of the polymer chemical structure (e.g., copolymerization or blending).[13,21,22]

Appropriate substitution can lead to soluble polymers allowing for processing by common methods including spin- or spray-coating. For instance, the presence of alkyl side chains increases the polymers' processability while modulating the electronic properties of the conjugated main chain. Introduction of strong electron-donating alkoxy side chains leads to polymers with low oxidation potentials and good stability in oxidized form.[23−31] In addition, the presence of alkoxy side chains lowers the steric hindrance in the surroundings of the main chain, resulting in planar, highly conjugated structures with low band gaps.[32,33] Moreover, ionic side chains (sulfonates, carboxylates, phosphonates, etc.) can be covalently bonded to the conjugated polymer backbone, resulting in water-soluble and self-doped materials.[34−50] For example, the presence of sulfonate groups on the polymer backbone confers the advantage of both anion and cation exchange properties.[51,52]

Extending our work in the field of PXDOPs,[53−55] here we report the synthesis and electrochemical and optical properties of several N-substituted PProDOPs. Our goal was to obtain materials with high band gaps while preserving a low oxidation potential for both monomer and resulting polymer. Substitution is known to provide a way of controlling the band gap,[56] as the presence of side chains induces a twist of the conjugated backbone, resulting in a decrease of the π-conjugation and therefore an increase of the band gap. PXDOPs with high

[†] University of Florida.
[‡] Istanbul Technical University.

10.1021/ma021108x CCC: $25.00
Published on Web 01/17/2003

Table 1. Electrochemical and Optical Properties of PProDOPs

polymer	$E_{ox/mon}$ (V) vs Fc/Fc$^+$	$E_{1/2}$ vs Fc/Fc$^+$ (V)	i_{pa}/i_{pc}[a]	ΔE_p[a] (mV)	λ_{max} (nm)	E_g (eV)
PProDOP	+0.58	−0.89	1.39	160	482/523	2.2
N-Me PProDOP	+0.50	−0.24	1.35	92	330	3.0
N-Pr PProDOP	+0.51	−0.16	1.02	8	306	3.4
N-Oct PProDOP	+0.52	−0.14	1.02	6		
N-Gly PProDOP	+0.54	−0.13	0.99	2	306	3.4
N-PrS PProDOP	+0.25	−0.10	0.98	6	340	2.9

[a] Scan rate: 20 mV/s.

band gaps are expected to have a $\pi-\pi^*$ transition in the UV and, therefore, give colorless materials in their neutral state. Upon application of a small voltage, the polymers can be switched to a doped colored state due to charge carrier absorptions induced in the visible region of the spectrum. These new polymers are expected to retain some of the electrochemical properties of the parent PProDOP such as a low oxidation potential, thus allowing their electropolymerization under milder conditions relative to unsubstituted polypyrroles. Moreover, judicious selection of substituents could lead to monomers with even lower oxidation potential than ProDOP due to an increased electron density at the redox center via inductive effects. These electroactive polymers are excellent candidates as anodically coloring materials in dual polymer electrochromic displays.[57,58] In addition to the required complementary optical properties, they possess a high degree of electrochemical compatibility with the PXDOT family of cathodically coloring polymers. This could lead to a new generation of ECDs exhibiting extremely high contrast over the entire visible region and long-lived switching capabilities.[59]

Results and Discussion

Monomer Synthesis. We have previously reported the synthesis and properties of 3,4-alkylenedioxypyrrole monomers and of the polymers derived therefrom.[53−55] In this study, N-substitution of 3,4-propylenedioxypyrrole (ProDOP) was performed through an N-alkylation with several alkyl chains having different lengths and hydrophilic/hydrophobic character (see Figure 1). ProDOP was treated with sodium hydride and alkyl bromides were added at room temperature. The reaction mixtures were refluxed for designated times, and purification by chromatography afforded the N-alkylated products **2a**−**c**. For **2d**, *tert*-butyldimethylsilyl (TBDMS)-protected tri(ethylene glycol) mesylate was added to a solution of ProDOP after treatment with sodium hydride. After the reaction was completed and purified, deprotection by tetrabutylammonium fluoride afforded *N*-Gly ProDOP. To obtain the sulfonated monomer **2e**, ProDOP was treated with NaH in dry THF and 1-propanesulfonate was subsequently added at room temperature. The reaction mixture was refluxed for 24 h, and purification afforded ProDOP-*N*-propylsodium sulfonate in 85% yield.[60]

Electrochemical Polymerization. Monomers **2a**−**d** were electropolymerized/deposited from solutions containing 10 mM monomer in 0.1 M $LiClO_4$/propylene carbonate (PC). Electropolymerization of **2e** was carried out in a mixture of PC and water (94:6). The presence of a small amount of water provides for the solubility of the monomer which is otherwise insoluble in acetonitrile (ACN), *N*,*N*-dimethylformamide (DMF), or PC. Table 1 shows the monomer's peak oxidation potentials ($E_{p,m}$) monitored during accumulative growth at a scan rate of 20 mV/s. Comparable to the relationship between pyrrole and *N*-alkyl pyrroles, the oxidation potential of ProDOP ($E_{ox,m}$ = +0.58 V vs Fc/Fc$^+$)[53−55] is higher than that of the N-substituted ProDOPs. The propylenedioxy substituent in the 3- and 4-positions of the pyrrole ring increases the electron-rich character of the monomer, thus leading to low monomer oxidation potentials. In addition, *N*-alkyl substitution increases the electron density at the redox center via inductive effects, and the resulting monomers possess even lower oxidation potentials than the parent ProDOP. The oxidation potential of the monomer minimally increases with the chain length (+0.50 V for *N*-Me ProDOP, +0.51 V for *N*-Pr ProDOP, +0.52 V for *N*-Oct ProDOP, and +0.54 V for *N*-Gly ProDOP vs Fc/Fc$^+$). The oxidation potential for monomer **2e** is lower than the other N-substituted ProDOPs (+0.25 V vs Fc/Fc$^+$). This could be due to the fact that *N*-PrS ProDOP forms more stable radical cations, the positive charge being balanced by the negatively charged sulfonate end group.

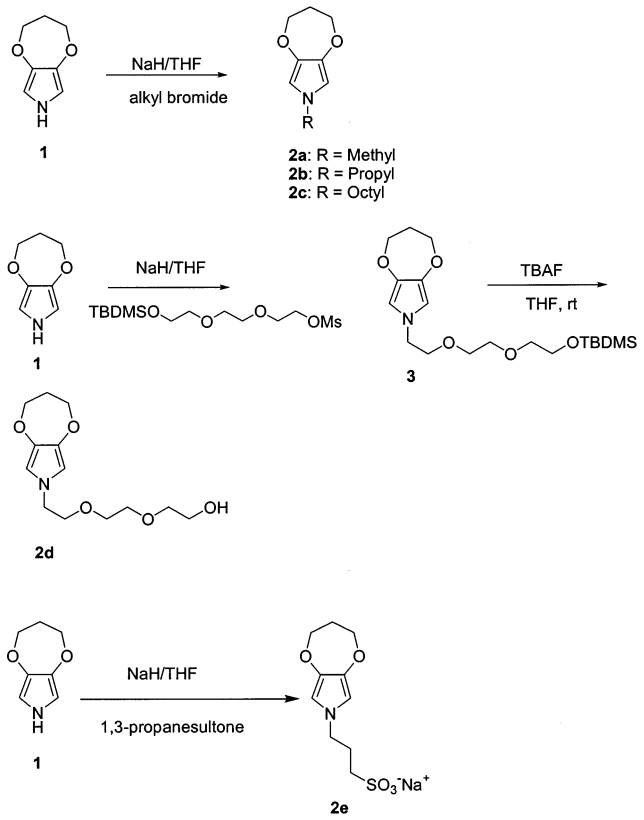

R	Products
CH_3	*N*-Me ProDOP (**2a**)
$(CH_2)_2CH_3$	*N*-Pr ProDOP (**2b**)
$(CH_2)_7CH_3$	*N*-Oct ProDOP (**2c**)
$(CH_2)_2O(CH_2)_2O(CH_2)_2OH$	*N*-Gly ProDOP (**2d**)
$(CH_2)_3SO_3Na$	*N*-PrS ProDOP (**2e**)

Figure 1. Synthesis of N-substituted ProDOPs.

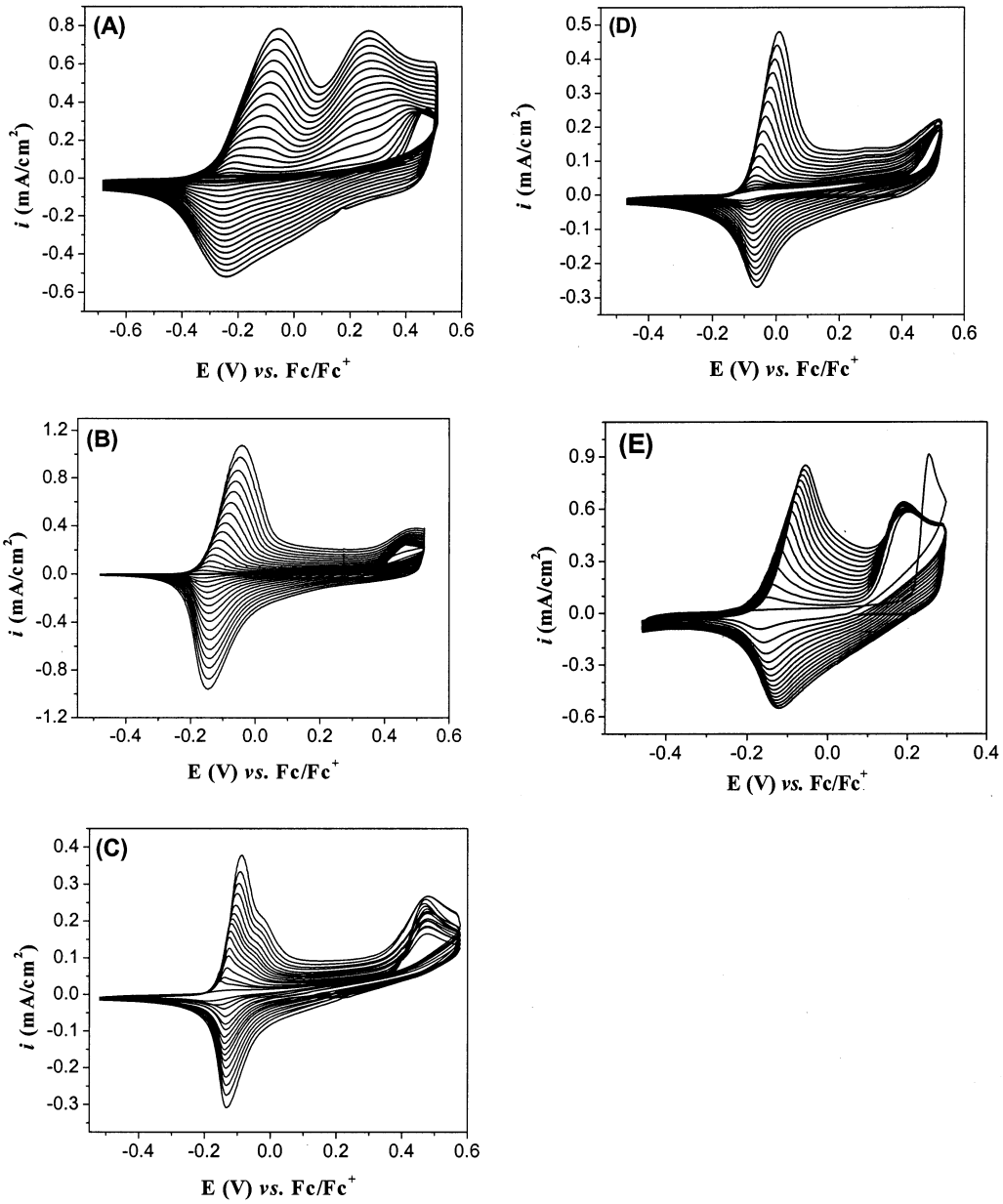

Figure 2. Potential scanning electrodeposition of *N*-alkyl ProDOPs from a 0.01 M solution of monomer in 0.1 M $LiClO_4$/PC at 20 mV/s on a Pt button electrode (area = 0.02 cm^2): (A) *N*-Me PProDOP (20 cycles), (B) *N*-Pr PProDOP (150 cycles), (C) *N*-Oct PProDOP (150 cycles), (D) *N*-Gly PProDOP (50 cycles), (E) *N*-PrS PProDOP (15 cycles).

Potentiodynamic polymerizations of monomers **2a**−**e** are shown in Figure 2. In all cases, the low potential polymer redox process is seen to evolve quite nicely. In the case of *N*-Me PProDOP polymerization (Figure 2A), the appearance of a peak distinct from the polymer redox process at a lower potential than monomer oxidation (+0.20 V vs Fc/Fc^+) may indicate a growth involving the coupling of soluble oligomers, which are more reactive than the monomer itself.[61] For monomers **2b** and **2c**, the polymerization proceeds at much slower rate. This substantial decrease of the electropolymerization rate has been reported previously for N-alkylated pyrroles and was attributed to a decrease in conductivity resulting from the N-substitution.[62] Usually, the longer the substituent, the lower the conductivity of the resulting film and therefore the slower its electrodeposition. For instance, after 20 cycles, the anodic peak current of *N*-Me PProDOP is about 0.80 mA/cm^2 while *N*-Pr PProDOP only reaches 0.054 mA/cm^2 and *N*-Oct PProDOP 0.050 mA/cm^2. Note that, despite a longer chain, *N*-Gly PProDOP and N-PrS ProDOP electrodepositions (Figure 2, D and E, respectively) are much faster than for the other *N*-alkyl PProDOPs, except *N*-Me PProDOP. This increase in the deposition rate is probably induced by the more hydrophilic character of the substituents, which provides a better adherence to the substrate. It is noteworthy that all of the polymers studied, with the exception of *N*-Me PProDOP, present very narrow redox processes during the accumulative growth. Since the half-wave oxidation potentials vary linearly with the inverse of the number of repeating units,[63] this seems to indicate that the resulting polymers have a narrow molecular weight distribution.

Polymer Characterization. The polymers were deposited by cyclic voltammetry on a platinum button electrode (area: 0.02 cm^2) from a 0.01 M solution of monomer in 0.1 M $LiClO_4$/PC electrolyte. To compare the electrochemical behavior of different N-substituted polymers, and since the rate of polymerization is much slower when the chain length is increased, the elec-

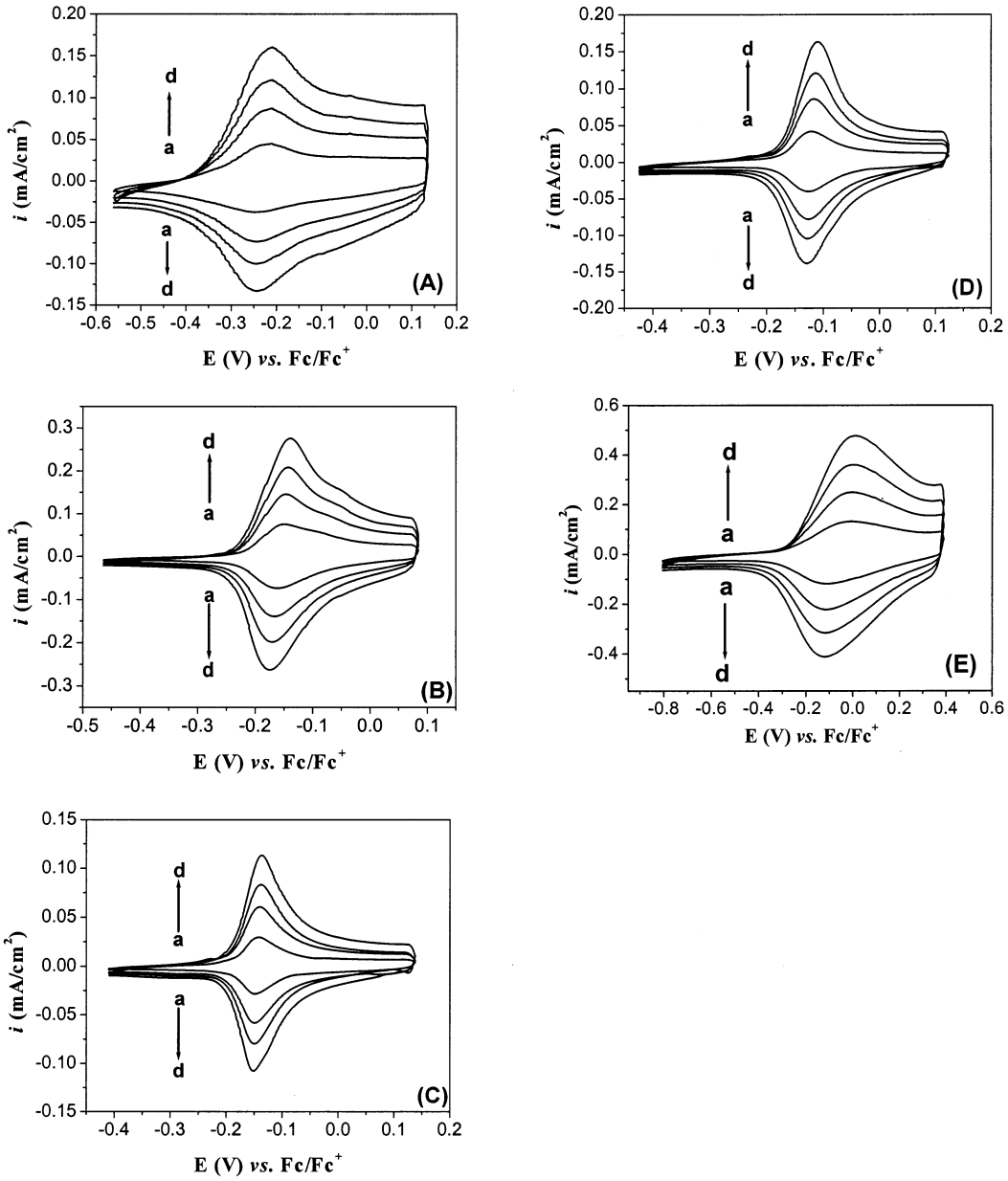

Figure 3. Cyclic voltammograms of thin *N*-alkyl PProDOP films in monomer-free solution of 0.1 M $LiClO_4$/PC: (A) *N*-Me PProDOP, (B) *N*-Pr PProDOP, (C) *N*-Oct PProDOP, (D) *N*-Gly PProDOP, (E) *N*-PrS PProDOP at a scan rate of (a) 50 mV/s, (b) 100 mV/s, (c) 150 mV/s, (d) 200 mV/s.

trodeposition was performed over 4 cycles for *N*-Me ProDOP, 5 cycles for *N*-Gly ProDOP, 20 cycles for *N*-Oct ProDOP, 40 cycles for *N*-Pr ProDOP, and galvanostatically for *N*-PrS ProDOP at a current density of 0.04 mA/cm^2 by passing a total charge of 10 mC/cm^2. As a result, all polymers are in a relatively narrow range of current densities.

Figure 3 shows cyclic voltammograms of N-substituted PProDOP thin films at scan rates of 50, 100, 150, and 200 mV/s in 0.1 M $LiClO_4$/PC. Very well-defined and reversible redox processes are seen with N-substituted PProDOPs, in contrast to the broad redox processes reported for *N*-alkyl pyrroles.[64] Half-wave oxidation potentials of the polymers ($E_{1/2}$) are between -0.10 and -0.25 V vs Fc/Fc$^+$ (see Table 1). As observed for the monomer oxidation potentials, the longer the N-substituent, the higher the $E_{1/2}$ (with *N*-PrS ProDOP being the exception), a phenomenon observed as well for *N*-alkyl pyrroles.[65] This could result from the substituent distorting the polymer backbone and decreasing the degree of conjugation. The capacitive behavior of these materials decreases with an increase in the N-substituent length. We attribute this to a drop in electronic conductivity as interchain interactions are decreased with increasing side chain length.

Figure 4 shows the CV of *N*-PrS PProDOP prepared in the absence of supporting electrolyte. Although we observed well-defined and reversible redox processes in the films prepared in the presence of (Figure 3E) and without electrolyte, the fact that the current densities are comparable at the same scan rates leads to the conclusion that the polymer is self-doping.[34,41,43]

To illustrate the outstanding reversibility of these redox processes, the anodic to cathodic peak current ratios (i_{pa}/i_{pc}) and the peak separation (ΔE_p) are reported in Table 1. With the exclusion of *N*-Me PProDOP, which exhibits a peak ratio of 1.35 and a relatively high peak separation (92 mV), all of the other N-substituted PProDOPs present an almost ideal ratio of 1.0 along with a very small ΔE_p (less than 8 mV) at a scan rate

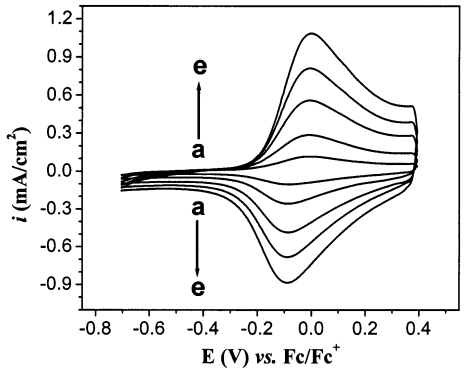

Figure 4. Cyclic voltammogram of a thin *N*-PrS PProDOP film in monomer-free solution of 0.1 M $LiClO_4$/PC. The polymer film was grown galvanostatically at a current density of 0.04 mA/cm^2 by passing a total charge of 20 mC/cm^2 from a 0.01 M monomer in PC:H_2O (94:6) without supporting electrolyte. Scan rates are (a) 20, (b) 50, (c) 100, (d) 150, and (e) 200 mV/s.

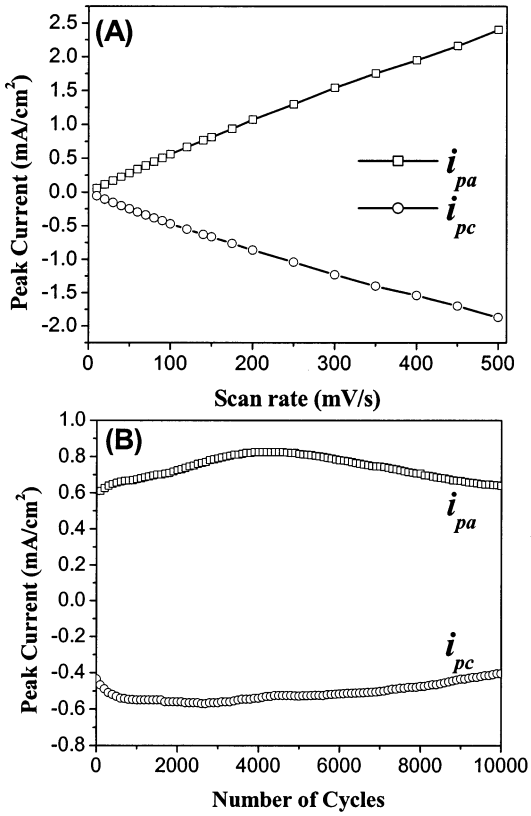

Figure 5. (A) Variation of anodic and cathodic peak currents as a function of the scan rate for a *N*-PrS PProDOP film in 0.1 M $LiClO_4$/CAN solution. (B) Variation of anodic (□) and cathodic (○) peak currents as a function of number of cycles for 0.12 μm thick *N*-PrS PProDOP film, cycled 10 000 times at a scan rate of 100 mV/s.

of 20 mV/s. The scan rate dependence of the anodic and cathodic peak currents shows a linear dependence as a function of the scan rate as illustrated in Figure 5A for *N*-PrS PProDOP. This demonstrates that the electrochemical processes are not diffusion limited and are reversible, even at very high scan rates. The ability to be switched reversibly in a non-diffusion-limited process at scan rates as high as 500 mV s^{-1} is rather unusual for conducting polymers and may stem from the thinness of the polymer films (about 30 nm). As seen in Table 1, ΔE_p decreases with increasing substituent length, and the anodic-to-cathodic peak ratio gets closer to 1.0, which indicates that the redox processes become more reversible. In summary, the N-substituted PProDOP electrochemistry shows very well-defined redox processes and outstanding reversibility as compared to polypyrrole and PProDOP.

The stability of the polymer for long-term switching between oxidized and neutral states is an important characteristic for the use of these materials in device applications. We monitored changes in the anodic and cathodic peak potentials and currents of a 0.12 μm *N*-PrS PProDOP film, prepared by galvanostatic deposition at a constant current density of 0.04 mA/cm^2. The film was cycled for 10 000 times with a scan rate of 100 mV/s in 0.1 M $LiClO_4$/PC. Figure 5B shows both the anodic and cathodic peak currents slowly increase during the first few thousand cycles. This is followed by a slow decrease, such that after 10 000 cycles the current response from the polymer is close to its initial value. The overall charge involved in the electrochemical process was calculated for each voltammogram, and the total charge change during this experiment decreases by less than 8% after 5000 cycles and less than 30% after 10 000 cycles. This shows that *N*-PrS PProDOP films are able to be switched many times between oxidized and reduced states with relatively small changes in electroactivity, making this polymer a good candidate for electrochromic applications.

Spectroelectrochemistry. N-Substituted PProDOP thin films were deposited on ITO/glass substrates using a galvanostatic deposition at a current density of 0.01 mA/cm^2. Electroactive *N*-Oct ProDOP thin films could be obtained on ITO/glass, but they were not thick enough to allow the spectroelectrochemical analysis, probably due to the strong monomer hydrophobicity conferred by the long alkyl chain. Figure 6 shows the spectroelectrochemistry of *N*-Me PProDOP (A), *N*-Pr PProDOP (B), *N*-Gly PProDOP (C), and *N*-PrS PProDOP (D) in 0.1 M $LiClO_4$/PC. As expected, the N-substitution has blue-shifted the π-to-π^* transition, which now lies in the UV range, with a λ_{max} at 330 nm (3.75 eV) for *N*-Me PProDOP, 340 nm (3.65 eV) for *N*-PrS PProDOP, and 306 nm (4 eV) for *N*-Pr PProDOP and *N*-Gly PProDOP. This corresponds to a band gap (measured at the edge of the π-to-π^* absorption band) of 3.0 eV for *N*-Me PProDOP, 2.9 eV for *N*-PrS PProDOP, and 3.4 eV for the other polymers, which are noticeably higher than that of PProDOP (2.2 eV).[53,55] The blue shift relative to PProDOP can be explained by the steric effect of the N-substituent. The ability to control the band gap with steric interaction is especially useful for electrochromic polymers as a broad range of colors can be easily obtained in a single polymer family. The significant blue shift obtained by adding an N-substituent to the ProDOP ring opens up the use of these materials as anodically coloring polymers, which are colorless in the neutral state and become colored upon doping, yet undergo their redox switch at a sufficiently low potential to yield the long lifetimes shown above. Neutral *N*-Gly PProDOP and *N*-PrS PProDOP absorb only in the UV range, thus causing them to be transparent and colorless while *N*-Me and *N*-Pr PProDOPs retain a residual coloration (e.g., light purple in the case of *N*-Me PProDOP).

Upon oxidation, the π-to-π^* transition is depleted at the expense of a broad and intense absorption band centered in the near-infrared (NIR), corresponding to the low-energy charge carriers. The tail of this NIR band

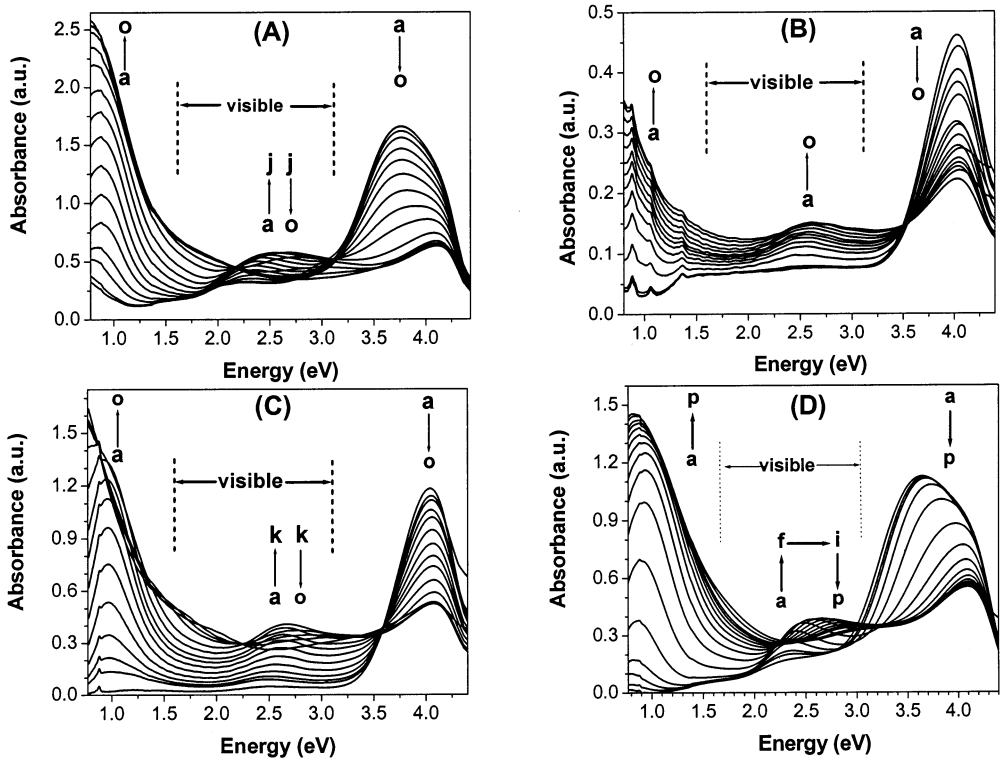

Figure 6. Spectroelectrochemistry of *N*-alkyl PProDOPs in 0.1 M $LiClO_4$/PC vs Fc/Fc^+: (A) *N*-Me PProDOP at applied potentials of (a) −500, (b) −400, (c) −300, (d) −275, (e) −250, (f) −230, (g) −200, (h) −160, (i) −120, (j) −75, (k) 0, (l) +100, (m) +300, (n) +500, (o) and +700 mV. (B) *N*-Pr PProDOP at applied potentials of (a) −400, (b) −300, (c) −200, (d) −150, (e) −100, (f) −80, (g) −60, (h) −40, (i) −20, (j) 0, (k) +50, (l) +100, (m) +200, (n) +400, (o) and +600 mV. (C) *N*-Gly PProDOP at applied potentials of (a) −200, (b) −70, (c) −60, (d) −50, (e) −40, (f) −30, (g) −20, (h) −10, (i) 0, (j) +20, (k) +60, (l) +200, (m) +300, (n) +400, (o) and +700 mV. (D) *N*-PrS PProDOP at applied potentials of (a) −0.40, (b) −0.30, (c) −0.25, (d) −0.20, (e) −0.15, (f) −0.10, (g) −0.05, (h) 0.00, (i) +0.05, (j) +0.10, (k) +0.15, (l) +0.20, (m) +0.25, (n) +0.30, (o) +0.40, and (p) +0.50 V.

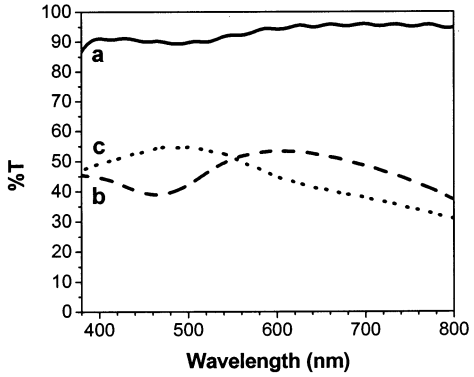

Figure 7. Transmittance of *N*-Gly PProDOP in the visible region as a function of wavelength (nm) for three different oxidation states: (a) neutral, (b) low doping level, and (c) high doping level.

as well as an intermediate band in the visible region is responsible for the coloration of the polymer films. The intensity of this coloration is, at best, moderate when compared to the neutral colored states of the PProDOP parent or the dioxythiophene polymers.

The visible light transmittance (%*T*) of *N*-Gly PProDOP at different doping levels is presented in Figure 7. In the neutral state (−300 mV vs Fc/Fc^+), the polymer film is highly transparent and transmits more than 90% of the light over the entire visible spectrum. At an intermediate potential (+60 mV), the transmittance shows a minimum of 40% at about 470 nm. When the polymer reaches its highest oxidation level (+700 mV), the transmittance below 550 nm increases at the expense of the transmittance at longer wavelengths. The transmittance minimum at 470 nm disappears and now corresponds to a maximum of the transmittance in the visible (about 55%). These changes in transmittance over the visible range of light have a great influence on the color of the polymer, which switches from a transparent colorless neutral state to a blue-doped state. *N*-Gly PProDOP is therefore a pure anodically coloring material, which is extremely rare among electrochromic polymers. On the other hand, with similar optical properties, *N*-PrS PProDOP has several advantages over *N*-Gly PProDOP. For instance, the deposition rate is much faster, the film quality is better, film conductivities are higher, and the colors obtained are more saturated.

Conductivity and Processability of *N*-PrS PProDOP. *N*-PrS PProDOP free-standing films were prepared by galvanostatic deposition on glassy carbon electrodes from solutions of PC and water (94:6) containing 0.01 M monomer with and without 0.1 M $LiClO_4$ at room temperature. Room temperature conductivities of these free-standing films were measured using the four point probe technique and found to be low, in the range of 10^{-4}−10^{-3} S/cm, in accordance with results reported in the literature for the N-substituted pyrrole derivatives.[66] The resulting polymer films were completely soluble in water in both their oxidized and neutral forms. Because of the electropolymerization method used, monomer consumption is quite low by design, making the polymer yields low. Even in the best instances, electropolymerization yields are on the order of 5−10%.

Electrochemically prepared *N*-PrS PProDOP free-standing films were dissolved in water and the solutions

Table 2. Potential-Dependent CIE 1931 *Yxy* and CIE 1976 *L*a*b Color Spaces for *N*-Me PProDOP, *N*-PrS PProDOP, and *N*-Gly PProDOP**

polymer	*E* (V) vs Fc/Fc$^+$	*Y* (%)	*L*	*a*	*b*	color
N-Me PProDOP	−1.10	25.9	58	11	0	deep purple
	−0.30	27.1	59	10	2	
	−0.15	28.7	60	4	8	
	0.00	30.1	62	−1	5	dark green
	+0.10	30.8	62	−3	3	
	+0.20	31.3	63	−3	0	
	+0.50	32.2	64	−4	−3	blue
	+0.70	31.7	63	−5	−4	
N-PrS PProDOP	−0.9	94.0	98	3	3	colorless
	−0.75	94.3	98	2	3	
	−0.20	91.1	96	5	2	pale pink
	0.00	74.1	89	13	0	pink
	+0.20	66.6	85	4	11	tan
	+0.40	62.3	83	−2	7	
	+0.50	61.3	83	−4	4	gray-green
	+0.70	58.7	81	−5	−1	
	+0.90	54.5	79	−4	−3	gray-blue
N-Gly PProDOP	−0.60	99.6	98	0	4	colorless
	−0.20	98.6	97	0	4	
	−0.10	90.2	94	2	4	pale pink
	0.00	61.3	81	1	12	pink/gray
	+0.20	58.9	79	−3	7	
	+0.30	58.9	79	−4	5	gray
	+0.40	58.9	79	−5	3	
	+0.50	58.9	79	−6	1	blue/gray
	+0.70	58.5	79	−6	−1	

subsequently cast onto glassy carbon button electrodes, followed by the evaporation of water. Cyclic voltammograms of these films in monomer-free organic electrolyte showed the polymer to be electroactive with CV response quite similar to that of the electrodeposited films, demonstrating that this polymer is processable and does not lose its electroactivity upon dissolution and subsequent reprecipitation.

To study the optical properties of aqueous solutions of *N*-PrS PProDOP, polymer films were prepared on a Pt foil working electrode from a solution of 0.01 M monomer in 0.1 M $LiClO_4$/PC:H_2O (94:6) using a current density of 0.04 mA/cm^2 and a charge density of 0.45 C/cm^2. The films were held at a neutralization potential (−0.7 V vs Ag/Ag$^+$) for 15 min, washed with ACN and acetone, dried under vacuum, and then subsequently dissolved in 3.0 mL water for spectral investigations. The neutral polymer solution showed a $\pi-\pi^*$ transition at 285 nm with an absorption onset of 3.45 eV. These values are blue-shifted with regard to the values obtained for thin solid films (see Table 1) as expected as the polymer chains can adopt more twisted average conformations. Similar shifts were reported by Patil et al. for poly(3-(alkanesulfonate)thiophene)s.[35]

Colorimetry. The results above demonstrate that *N*-Me, *N*-PrS, and *N*-Gly PProDOPs have unique electrochemical and optical properties. As color is the most important property for consideration in electrochromic applications, we studied the above polymers by colorimetry and express the results in the CIE 1931 *Yxy* and CIE 1976 *L*a*b** color spaces as recommended by the "Commission Internationale de l'Eclairage" (CIE).[67,68] The colors observed for each polymer at different doping levels are summarized in Table 2. Upon oxidation, *N*-Me PProDOP changes from purple to blue through a dark green intermediate. It should be noted that a deep purple color does not have a single dominant wavelength located on the spectral locus of the CIE 1931 diagram and results from the addition of several absorptions located at different wavelengths in the visible spectrum.[69] The color track of this polymer in the CIE 1931 *Yxy* color space is shown in Figure 8A. Between −1.10 and −0.30 V vs Fc/Fc$^+$, the *xy* coordinates are almost invariant, signifying no visible change in the color of the polymer. When the potential is stepped up to +0.85 V, the dominant wavelength of the light transmitted through the material decreases as a result of charge carrier formation, showing absorptions at longer wavelengths. At higher potentials, the transitions associated with the charge carriers decrease in intensity, as shown by spectroelectrochemistry, thus resulting in a lower absorption at longer wavelengths and therefore a decrease of the dominant wavelength. This behavior is quite typical for electrochromic polymers, as we reported previously.[67] The color tracks of *N*-Gly PProDOP and *N*-PrS PProDOP, shown in Figure 8, B and C, respectively, present similar features. However, the *xy* coordinates of these polymers in the neutral state are in the proximity of the white point ($x = 0.349$, $y = 0.378$), indicating that the materials are colorless. As seen in Table 2, *N*-Gly PProDOP and *N*-PrS PProDOP change upon oxidation from colorless to blue-gray through different shades including light pink and gray. These

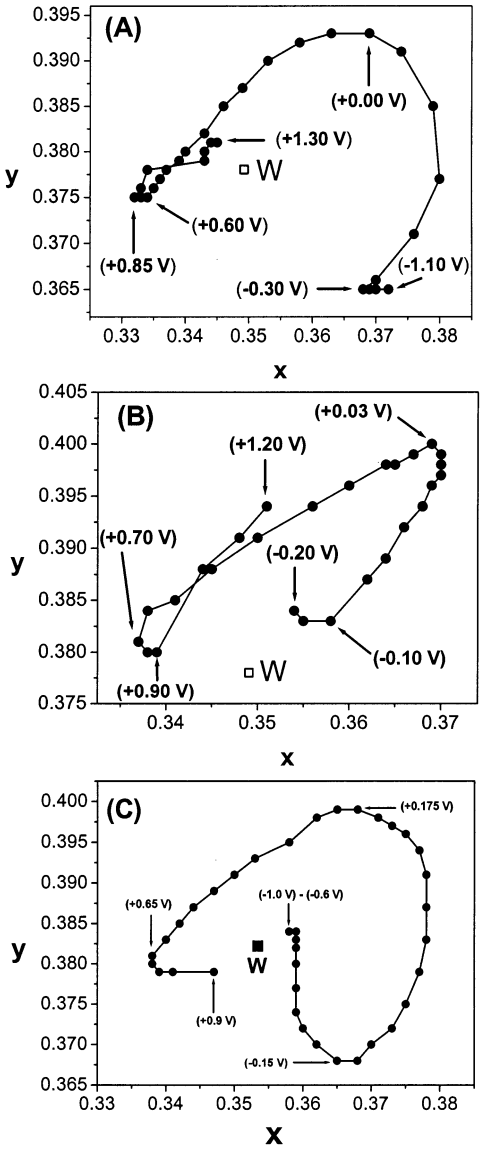

Figure 8. Colorimetry ($x-y$ diagram) of (A) *N*-Me PProDOP, (B) *N*-Gly PProDOP, and (C) *N*-PrS PProDOP.

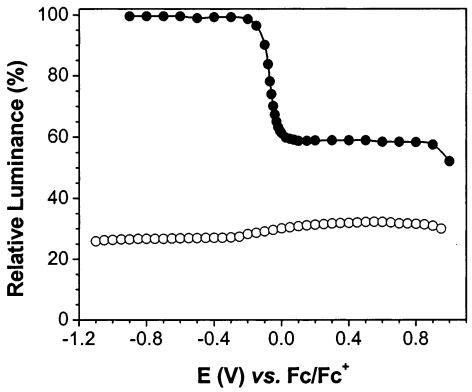

Figure 9. Relative luminance of *N*-Me PProDOP (○) and *N*-Gly PProDOP (●) as a function of the potential applied vs Fc/Fc^+.

colors are quite different from those observed in PProDOP, which switches from orange to light blue-gray through brown.[55]

The luminance, which is a coordinate in the *Yxy* color space, represents the brightness of a color as seen by the human eye. It is also very informative since with only one value, it provides information about the perceived transparency of a sample over the entire visible range of light. %Y is different from %T (single wavelength) as it takes into account the full spectrum and light sensitivity of the human eye, which is not constant over the entire visible range.[67,70] Relative luminance (%Y) changes of *N*-Me and *N*-Gly PProDOP are presented in Figure 9. Again, the behavior of these polymers is different from that of PProDOP, which has a lower luminance when neutral than in the doped state and also presents a minimum at intermediate potentials (darkest state corresponding to a brown color). *N*-Me PProDOP shows a slightly lower luminance in the neutral state (27%) than in the doped state (32%), but the response is relatively featureless. As emphasized previously, the behavior of *N*-Gly PProDOP is quite exceptional for an electrochromic polymer and is confirmed by the luminance measurements, which show that the polymer film has a luminance of almost 100% in the neutral state, corresponding to a colorless and completely transparent material. The luminance remains almost unchanged when the potential is stepped up to −0.20 V vs Fc/Fc^+, then decreases abruptly to about 55% at −0.10 V, and stabilizes at this value up to +0.85 V vs Fc/Fc^+. The difference in behavior between *N*-Gly PProDOP and *N*-Me PProDOP is closely related to their relative band gaps. In fact, the π-to-π^* transition in *N*-Gly PProDOP is entirely located in the UV range, and even the tail of this transition does not overlap with the visible range of light. As a result, the depletion of the π-to-π^* transition has no effect on the color of the polymer. Therefore, only the transitions associated with the charge carriers give rise to a visible color. *N*-PrS ProDOP shows similar behavior. The ability to switch between a colorless neutral state and a doped blue-gray state confers to these electrochromics the rare property of being truly anodically coloring.

Conclusions

In summary, a series of N-substituted PProDOPs has been prepared showing reversible and long-lived electrochemistry, along with useful electrochromic properties. Low half-wave oxidation potentials confer a high degree of stability in the doped state since air and moisture are not likely to reduce the oxidized forms. The N-substitution allows a fine-tuning of the band gap and therefore of the optical properties of the resulting materials. The ability to design and synthesize pure anodically coloring polymers has been demonstrated with *N*-PrS and *N*-Gly PProDOP. The ease with which these new compounds can be derivatized opens up a wide range of possibilities for the production of advanced polymers for display applications including electrochromic devices. In particular, the introduction of proper substituents on the propylenedioxy ring led to soluble and self-doping anodically coloring polymers, which might be of high interest for processable electrochromics in display applications.

Experimental Section

All chemicals were purchased from Aldrich Chemical. Propylene carbonate (99.8%, anhydrous) was distilled over calcium hydride before use. Sodium hydride was used as purchased. Tetrahydrofuran (THF) was freshly distilled over sodium/benzophenone. All monomers were synthesized following a published procedure.[60] ^1H NMR and ^{13}C NMR were recorded on QE-300 (300 MHz, General Electric Co.) spectrometer. Infrared spectroscopy was recorded on a Biorad FTS-40 FTIR. Mass spectrometry was carried out on a Finnigan MAT 95Q mass spectrometer. Film thicknesses were measured with a Dektak 3030 profilometer over several points of the sample to yield an average thickness.

Electropolymerization was carried out with an EG&G Princeton Applied Research model 273 potentiostat/galvanostat employing a platinum button working electrode (diameter 1.6 mm; area 0.02 cm^2), a platinum flag counter electrode and a calibrated silver wire or 0.01 M $Ag/AgNO_3$ reference (Ag/Ag^+). The electrolyte used was 0.1 M $LiClO_4$/PC. The reference was calibrated externally using a 5 mM solution of ferrocene (Fc/Fc^+) in the same electrolyte ($E_{1/2}(Fc/Fc^+) = +0.070$ V vs Ag/Ag^+ in 0.1 M $LiClO_4$/PC). The potentials were calibrated vs Fc/Fc^+ in the same electrolyte, as recommended by IUPAC.[71] All potentials are reported vs Fc/Fc^+. The electrodeposition was performed from a 0.01 M solution of monomer in the electrolyte at a scan rate of 20 mV/s. Cyclic voltammetry was carried out using the same electrode setup and using 0.1 M $LiClO_4$/PC electrolyte. Corrware II software from Scribner Associates was used for data acquisition and potentiostat control.

Spectroelectrochemical measurements were carried out using a Varian Cary 5E UV−vis−NIR spectrophotometer connected to a computer at a scan rate of 600 nm/min. A three-electrode cell assembly was used where the working electrode was an ITO-coated glass (7 × 50 × 0.6 mm, 10 Ω/□, Delta Technologies Inc.), the counter was a platinum wire, and a 0.01 M $Ag/AgNO_3$ was the reference electrode. The potentials were applied using the same EG&G potentiostat as previously described, and the data were recorded with Corrware II software for electrochemical data and with the Varian Cary Win-UV for spectral data.

Colorimetry measurements were obtained using a Minolta CS-100 chroma meter and CIE recommended normal/normal (0/0) illuminating/viewing geometry for transmittance measurements.[70] As for spectroelectrochemistry, a three-electrode cell was employed. The potential was controlled by the same EG&G potentiostat. The sample was illuminated from behind by a D50 (5000 K) light source in a light booth designed to exclude external light. The color coordinates are expressed in the CIE 1931 *Yxy* color space where the *Y* value is a measure of the luminance in Cd/m^2. The relative luminance, expressed in %, was calculated by dividing the *Y* value measured on the sample by the Y_0 value corresponding to the background. Note that the relative luminance is frequently reported instead of the luminance because it gives a more meaningful value.[72]

Polymer films for spectroelectrochemistry were prepared by galvanostatic deposition on ITO ($R_s \leq 10$ Ω/□). ITO supported

films were electrodeposited at 0.01 mA/cm^2 in 0.1 M $LiClO_4$/PC containing 0.01 M of monomer.

Acknowledgment. We gratefully acknowledge the financial support of the AFOSR (F49620-00-1-0047) and the ARO/MURI program (DAAD19-99-1-0316). We also thank Istanbul Technical University and the Scientific and Technical Research Council of Turkey (TUBITAK) for supporting the work of Gürsel Sönmez at the University of Florida through the NATO A-2 Science Fellowships Program.

References and Notes

(1) Deb, S. K. *Appl. Opt. Suppl.* **1969**, *3*, 192.
(2) Monk, P. M. S.; Mortimer, R. J.; Rosseinsky, D. R. *Electrochromism: Fundamentals and Applications;* VCH: Weinheim, 1995.
(3) Granqvist, C. G.; Azens, A.; Isidorsson, J.; Kharrazi, M.; Kullman, L.; Lindstroem, T.; Niklasson, G. A.; Ribbing, C.-G.; Roennow, D.; Stromme Mattsson, M.; Veszelei, M. *J. Non-Cryst. Solids* **1997**, *218*, 273.
(4) Monk, P. M. S. *J. Electroanal. Chem.* **1997**, *432*, 175.
(5) Bange, K. *Solar Energy Mater. Solar Cells* **1999**, *58*, 1.
(6) Granqvist, C. G.; Azens, A.; Hjelm, A.; Kullman, L.; Niklasson, G. A.; Ribbing, C.-G.; Roennow, D.; Stromme Mattsson, M.; Veszelei, M.; G. Vaivars *Solar Energy* **1998**, *63*, 199.
(7) Agnihotry, S. A.; Pradeep; Sekhon, S. S. *Electrochim. Acta* **1999**, *44*, 3121.
(8) Rauh, R. D. *Electrochim. Acta* **1999**, *44*, 3165.
(9) Tracy, C. E.; Zhang, J.-G.; Benson, D. K.; Czanderna, A. W.; Deb, S. K. *Electrochim. Acta* **1999**, *44*, 3195.
(10) Pennisi, A.; Simone, F.; Barletta, G.; Di Marco, G.; Lanza, L. *Electrochim. Acta* **1999**, *44*, 3237.
(11) Meeker, D. L.; Mudigonda, D. S. K.; Osborn, J. M.; Loveday, D. C.; Ferraris, J. P. *Macromolecules* **1998**, *31*, 2943.
(12) Mudigonda, D. S. K.; Meeker, D. L.; Loveday, D. C.; Osborn, J. M.; Ferraris, J. P. *Polymer* **1999**, *40*, 3407.
(13) Brotherson, I. D.; Mudigonda, D. S. K.; Ocborn, J. M.; Belk, J.; Chen, J.; Loveday, D. C.; Boehme, J. L.; Ferraris, J. P.; Meeker, D. L. *Electrochim. Acta* **1999**, *44*, 2993.
(14) Byker, H. J. Gentex Corporation, US Patent No. 4902108.
(15) Mortimer, R. G. *Chem. Soc. Rev.* **1997**, *26*, 147.
(16) Mortimer, R. J. *Electrochim. Acta* **1999**, *44*, 2971.
(17) De Paoli, M.-A.; Casabollore-Miceli, G.; Girotto, E. M.; Gazotti, W. A. *Electrochim. Acta* **1999**, *44*, 2983.
(18) Mastrogostino, M. *Applications of Electroactive Polymers*; Scrosati, B., Ed.; Chapman and Hall: London, 1993.
(19) Sapp, S. A.; Sotzing, G. A.; Reynolds, J. R. *Chem. Mater.* **1998**, *10*, 2101.
(20) Kumar, A.; Welsh, D. M.; Morvant, M. C.; Piroux, F.; Abboud, K. A.; Reynolds, J. R. *Chem. Mater.* **1998**, *10*, 896.
(21) Skotheim, T. A.; Elsenbaumer, R. L.; Reynolds, J. R. *Handbook of Conducting Polymers*, 2nd ed.; Marcel Dekker: New York, 1998.
(22) Nalwa, H. S. *Handbook of Organic Conductive Molecules and Polymers*; John Wiley and Sons: New York, 1997.
(23) Feldhues, M.; Mecklenburg, T.; Wegener, P.; Kampf, G. *Synth. Met.* **1989**, *28*, C487.
(24) Leclerc, M.; Daoust, G. *J. Chem. Soc., Chem. Commun.* **1990**, 273.
(25) Daoust, G.; Leclerc, M. *Macromolecules* **1991**, *21*, 455.
(26) Heywang, G.; Jonas, F. *Adv. Mater.* **1992**, *4*, 116.
(27) Faid, K.; Cloutier, R.; Leclerc, M. *Macromolecules* **1993**, *23*, 2501.
(28) Hong, Y.; Miller, L. L. *Chem. Mater.* **1995**, *7*, 1999.
(29) Zotti, G.; Gallazi, M. C.; Zerbi, G.; Meille, S. V. *Synth. Met.* **1995**, *8*, 769.
(30) Sotzing, G. A.; Reynolds, J. R.; Steel, P. J. *Chem. Mater.* **1996**, *8*, 882.
(31) Havinga, E. E.; Mutsaers, C. M. J.; Jenneskens, L. W. *Chem. Mater.* **1996**, *8*, 769.
(32) Inganas, O. *Trends Polym. Sci.* **1994**, *2*, 189.
(33) Hanna, R.; Leclerc, M. *Chem. Mater.* **1996**, *8*, 1512.
(34) Patil, A. O.; Ikonoue, Y.; Wudl, F.; Heeger, A. J. *J. Am. Chem. Soc.* **1987**, *109*, 1858.
(35) Patil, A. O.; Ikenoue, Y.; Colaneri, H.; Chen, J.; Wudl, F.; Heeger, A. J. *Synth. Met.* **1987**, *20*, 151.
(36) Ikenoue, Y.; Chiang, J.; Patil, A. O.; Wudl, F.; Heeger, A. J. *J. Am. Chem. Soc.* **1988**, *110*, 2983.
(37) Ikenoue, Y.; Uotani, N.; Patil, A. O.; Wudl, F.; Heeger, A. J. *Synth. Met.* **1989**, *30*, 305.
(38) Reynolds, J. R.; Sundaresan, N. S.; Pomerantz, M.; Basak, S.; Baker, C. K. *J. Electroanal. Chem.* **1988**, *250*, 355.
(39) Qiu, Y.-J.; Reynolds, J. R. *J. Electrochem. Soc.* **1990**, *137*, 900.
(40) Ikenoue, Y.; Tomozawa, H.; Saida, Y.; Kira, M.; Yashima, H. *Synth. Met.* **1991**, *40*, 333.
(41) Hou, C.-N.; Hua, M.-Y.; Chen, S.-A. *Mater. Chem. Phys.* **1994**, *36*, 359.
(42) Wudl, F.; Heeger, A. J. U.S. Patent 5,367,041, 1994.
(43) Chen, S.-A.; Hwang, G.-W. *J. Am. Chem. Soc.* **1995**, *117*, 10055.
(44) Nguyen, M. T.; Leclerc, M.; Diaz, A. F. *Trends Polym. Sci.* **1995**, *3*, 186.
(45) Aldissi, M. *Mol. Cryst. Liq. Cryst.* **1988**, *160*, 121.
(46) Tang, H.; Yamashita, T.; Kitana, A.; Ito, S. *Electrochim. Acta* **1998**, *43*, 2237.
(47) Chan, H. S. O.; Ho, P. K. H.; Ng, S. C.; Tan, B. T. G.; Tan, K. L. *J. Am. Chem. Soc.* **1995**, *117*, 8517.
(48) Barbero, C.; Kötz, R. *Adv. Mater.* **1994**, *6*, 577.
(49) Delabouglise, D.; Garnier, F. *New J. Chem.* **1991**, *15*, 233.
(50) Ng, S. C.; Chan, H. S. O.; Huang, H. H.; Ho, P. K. H. *J. Chem. Soc., Chem. Commun.* **1995**, 1327.
(51) Zhong, C.; Storck, W.; Doblhofer, K. *J. Phys. Chem.* **1990**, *94*, 1149.
(52) Bidan, G.; Ehui, B.; Lapkowski, M. *J. Phys. D*: *Appl. Phys.* **1988**, *21*, 1043.
(53) Thomas, C. A.; Zong, K.; Schottland, P.; Reynolds, J. R. *Adv. Mater.* **2000**, *12*, 222.
(54) Gaupp, C. L.; Zong, K.; Schottland, P.; Thomas, C. A.; Reynolds, J. R. *Macromolecules* **2000**, *33*, 1132.
(55) Schottland, P.; Zong, K.; Gaupp, C. L.; Thomson B. C.; Thomas, C. A.; Giurgiu, I.; Hickman, R.; Reynolds, J. R. *Macromolecules* **2000**, *33*, 7051.
(56) Roncali, J. *Chem. Rev.* **1997**, *97*, 173.
(57) Sapp, S. A.; Sotzing, G. A.; Reddinger, J. L.; Reynolds, J. R. *Adv. Mater.* **1996**, *8*, 808.
(58) Sapp, S. A.; Sotzing, G. A.; Reynolds, J. R. *Chem. Mater.* **1998**, *10*, 2101.
(59) Schwendeman, I.; Hickman, R.; Sonmez, G.; Schottland, P.; Zong, K.; Welsh, D. M.; Reynolds, J. R. *Chem. Mater.* **2002**, *14*, 3118.
(60) Zong, K.; Reynolds, J. R. *J. Org. Chem.* **2001**, *66*, 6873.
(61) Zotti, G.; Schiavon, G.; Berlin, A.; Pagani, G. *Chem. Mater.* **1993**, *5*, 430.
(62) Waltman, R. J.; Bargon, J. *Can. J. Chem.* **1986**, *64*, 76.
(63) Zotti, G.; Martina, S.; Wegner, G.; Schlüter, A. D. *Adv. Mater.* **1992**, *4*, 798.
(64) Diaz, A. F.; Castello, J.; Logan, J. A.; Lee, W. Y. *J. Electroanal. Chem.* **1981**, *129*, 115.
(65) Diaz, A. F.; Bargon, J. In *Handbook of Conducting Polymers*, 1st ed.; Skotheim, T. J., Ed.; Marcel Dekker: New York, 1986; Vol. I, p 81.
(66) Diaz, A. F.; Castillo, J. I.; Logan, J. A.; Lee, W.-Y. *J. Electroanal. Chem.* **1981**, *129*, 115.
(67) Thompson, B. C.; Schottland, P.; Zong, K.; Reynolds, J. R. *Chem. Mater.* **2000**, *12*, 1563.
(68) CIE; *Colorimetry* (Official Recommendations of the International Commission on Illumination), CIE Publication No. 15, Paris, 1971.
(69) Wyszecki, G.; Stiles, W. S. *Color Science*; Wiley: New York, 1982.
(70) Nassau, K. *Color for Science, Art and Technology*; Elsevier: Amsterdam, 1998.
(71) Gritzner, G.; Kuta, G. *J. Pure Appl. Chem.* **1984**, *56*, 461.
(72) Overheim, R. D.; Wagner, D. L. *Light and Color*; Wiley: New York, 1982; p 77.

MA021108X